Catalysis Today 143 (2009) 282–285

Contents lists available at ScienceDirect

Catalysis Today

journal homepage: www.elsevier.com/locate/cattod

Theoretical investigation of the interaction between oxygen molecules and small Au clusters using approximately spin-projected geometry optimization (AP-opt) method

M. Okumura [a,b,*], Y. Kitagawa [a], H. Yabushita [a], T. Saito [a], T. Kawakami [a]

[a] Graduate School of Science, Osaka University, 1-1 Machikaneyamacho, Toyonaka, Osaka 560-0043, Japan
[b] Core Research for Environmental Science and Technology (CREST), Japan Science and Technology Agency, Kawaguchi-shi, Saitama 332-0012, Japan

ARTICLE INFO

Article history:
Available online 4 January 2009

Keywords:
Au cluster
AP-opt method
DFT

ABSTRACT

The effects of spin contamination errors in the optimized geometry of oxygen-adsorbed Au cluster model systems were examined by using broken symmetry geometry optimization (BS-opt) and an approximate spin-projected broken symmetry geometry optimization (AP-opt) method combined with the hybrid density functional (B3LYP) method. The AP-opt method effectively eliminated spin contamination errors from the BS-opt calculations of optimized geometry and energy of Au_n–O_2 (n = 1, 2 and 13) model systems.

1. Introduction

In recent years, environmental catalysts have attracted interest due to increased social demands for pollutant control. Au is a promising material for environmental catalysis as it exhibits unique catalytic properties at low temperatures [1–4].

In previous work, we observed that CO strongly adsorbed onto the surface of Au clusters [5]. This raised the possibility that a key factor enabling the catalytic oxidation reaction with Au catalysts was the activation of O_2 molecules [6]. Recently, Tsukuda found that Au nanoclusters stabilized by poly(*N*-vinyl-2-pyrrolidone) [PVP; $(C_6H_9ON)_n$], abbreviated as Au:PVP, can selectively oxidize p-hydroxybenzyl alcohol into the corresponding aldehyde in water without degradation [7,8]. In this work, the control of cluster size, such the ability to prepare sub-nanometer clusters, becomes much more important since the size effect on the catalytic activity of Au cluster catalysts is significant. It is also well known that the electronic states of such clusters are not band structures but are discrete molecular orbital structures. Additionally, very small clusters can often have open-shell electronic states.

Recently, the broken symmetry density functional theory (BS DFT) method has been successfully applied to various metalloproteins containing transition metals [9]. The broken symmetry method can approximately involve the static correlation correction related to bond dissociation by α and β electrons into two different orbitals, namely the different orbitals for different spins (DODS) approach. Therefore, BS DFT calculations employ both dynamic and non-dynamic (static) correlation effect at lower computational costs than other *ab initio* methods such as MRMP2 and CASPT2. It is, however, well known that the BS procedure causes a crucial problem called the spin contamination error, where a solution in an open shell low spin (LS) state is contaminated by higher spin states [10,11,16]. Due to this error, it can be presumed that calculated characteristics for the LS state will be affected by those of the higher spin states. Yamaguchi et al. have proposed an approximate spin-projection (AP) method in order to eliminate the spin contamination error from the total energy of the BS LS state [12,13].

In previous papers, our group proposed a geometry optimization procedure based on the AP method, called the AP-opt method [14,15]. By using AP-opt, one can optimize structures without introducing spin contamination error. In this paper, we discuss the application of the AP-opt method to Au_n–O_2 (n = 1, 2 and 13) model systems, since the calculated geometries and energies of these model systems by BS DFT are known to contain large spin contamination errors.

2. Theoretical background of AP-opt method and computational details

The AP procedure proposed by Yamaguchi et al. introduces a Heisenberg Hamiltonian [17,18] to eliminate spin contamination error:

$$\hat{H} = -2\sum_{a>b} J_{ab}\hat{S}_a\hat{S}_b, \tag{1}$$

* Corresponding author at: Graduate School of Science, Osaka University, 1-1 Machikaneyamacho, Toyonaka, Osaka 560-0043, Japan.
E-mail address: ok@chem.sci.osaka-u.ac.jp (M. Okumura).

0920-5861/$ – see front matter © 2008 Elsevier B.V. All rights reserved.
doi:10.1016/j.cattod.2008.11.016

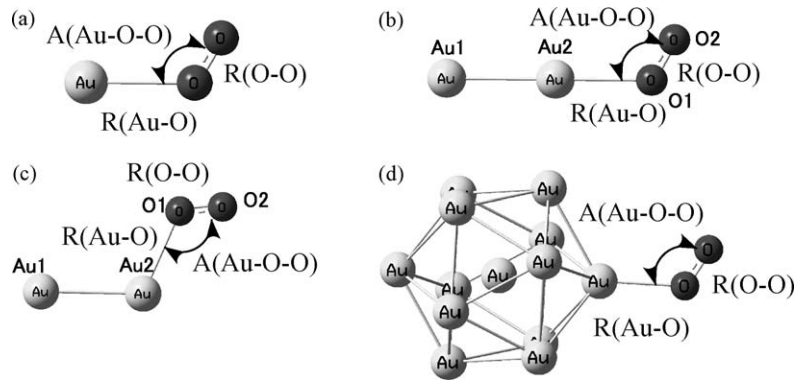

Fig. 1. Calculated structures of model clusters: (a) Au–O_2, (b) Au_2–O_2 type I, (c) Au_2–O_2 type II, and (d) Au_{13}–O_2.

where $\hat{S}_a$ and $\hat{S}_b$ are spin operators for spin sites a and b, and J_{ab} is an effective exchange integral. By using the simple approximations that the spin contamination in a high spin (HS) state is negligible and the spin densities of each spin site of the low spin state are equal to those of the HS state, a spin-projected total energy of the BS LS state can be derived as follows:

$$E^{\mathrm{LS}}_{\mathrm{APBS}} = \alpha E^{\mathrm{LS}}_{\mathrm{BS}} - \beta E^{\mathrm{HS}}_{\mathrm{BS}}, \tag{2}$$

where

$$\alpha = \frac{\langle \hat{S}^2 \rangle^{\mathrm{HS}}_{\mathrm{BS}} - \langle \hat{S}^2 \rangle^{\mathrm{LS}}_{\mathrm{exact}}}{\langle \hat{S}^2 \rangle^{\mathrm{HS}}_{\mathrm{BS}} - \langle \hat{S}^2 \rangle^{\mathrm{LS}}_{\mathrm{BS}}}, \tag{3a}$$

$$\beta = \frac{\langle \hat{S}^2 \rangle^{\mathrm{LS}}_{\mathrm{BS}} - \langle \hat{S}^2 \rangle^{\mathrm{LS}}_{\mathrm{exact}}}{\langle \hat{S}^2 \rangle^{\mathrm{HS}}_{\mathrm{BS}} - \langle \hat{S}^2 \rangle^{\mathrm{LS}}_{\mathrm{BS}}}, \tag{3b}$$

$$\beta = \alpha - 1. \tag{3c}$$

Generally speaking, the spin contamination error of the lowest spin state (e.g. the singlet state) is mainly derived from the lowest higher spin state (e.g. the triplet state). Our previous work demonstrated that the projected energies, such as an excitation energy, for the lowest spin state BS calculation results calculated by the approximate spin-projection method were in good agreement with experimental results [10]. Therefore, we presumed that the approximate spin-projection method was also applicable to the geometry optimization in the BS calculations. The gradient of $E^{\mathrm{LS}}_{\mathrm{APBS}}$, which is necessary for the geometry optimization, is given in the AP procedure as follows [14,15]:

$$\begin{aligned} G^{\mathrm{LS}}_{\mathrm{APBS}}(R) &= \frac{\partial E^{\mathrm{LS}}_{\mathrm{APBS}}(R)}{\partial R} \\ &= \{\alpha(R) G^{\mathrm{LS}}_{\mathrm{BS}}(R) - \beta(R) G^{\mathrm{HS}}_{\mathrm{BS}}(R)\} + \frac{\partial \alpha(R)}{\partial R}\{E^{\mathrm{LS}}_{\mathrm{BS}}(R) \\ &\quad - E^{\mathrm{HS}}_{\mathrm{BS}}(R)\}. \end{aligned} \tag{4}$$

It is difficult to calculate the derivative of α because it contains $\langle \hat{S}^2 \rangle$. By introducing the simple approximation that the spin contamination is negligible for the HS state, however, it can be reduced as follows:

$$\frac{\partial \alpha(R)}{\partial R} = \frac{\langle \hat{S}^2 \rangle^{\mathrm{HS}}_{\mathrm{BS}} - \langle \hat{S}^2 \rangle^{\mathrm{LS}}_{\mathrm{exact}}}{(\langle \hat{S}^2 \rangle^{\mathrm{HS}}_{\mathrm{BS}} - \langle \hat{S}^2 \rangle^{\mathrm{LS}}_{\mathrm{BS}})^2} \frac{\partial \langle \hat{S}^2 \rangle^{\mathrm{LS}}_{\mathrm{BS}}}{\partial R}. \tag{5}$$

Our group has proposed a numerical fitting procedure to obtain an approximate function of $\partial \langle \hat{S}^2 \rangle^{\mathrm{LS}}_{\mathrm{BS}} / \partial R$, which makes it possible to obtain the term $\partial \alpha(R)/\partial R$ [14,15,19]. The accuracy of this numerical approach was evaluated in the previous papers [14,15]. Using the AP-opt method, we successfully removed the spin contamination in all cases examined. Therefore, the calculated $\langle S^2 \rangle$ values coincided exactly with the theoretical values for the spin multiplicities handled. Our AP optimization was carried out using a custom-made program.

Unrestricted hybrid DFT (UB3LYP) calculations were carried out for model clusters. The model systems examined are depicted in Fig. 1. The LANL2DZ basis set was used for Au atoms and the 6-31+G* basis set was used for O atoms in O_2 molecules. All geometries of Au–O_2 and Au_2–O_2 model systems were fully optimized with C_1 symmetry. The Au_{13}–O_2 model cluster was partially optimized with C_1 symmetry using the UB3LYP method, where the geometry of the Au_{13} cluster was fixed. In the geometry optimization calculations for Au_2–O_2 and Au_{13}–O_2 models, several initial structures were used in order to search for their most stable optimized geometries. The Mulliken charges of each atom were calculated by Mulliken population analysis. All calculations were carried out by the Gaussian03 program [20].

3. Results and discussion

The ground sates of isolated Au atoms and O_2 molecules are doublet and triplet, respectively, and the calculated spin state of Au–O_2 model is doublet. The obtained $\langle S^2 \rangle$ of the Au–O_2 model by the broken symmetry geometry optimization (BS-opt) by B3LYP was 1.4509, while the exact $\langle S^2 \rangle$ value is 0.75. This demonstrates the large spin contamination error present in the Au–O_2 model system. On the other hand, there was no spin contamination error in the resulting $\langle S^2 \rangle$ values for isolated Au atoms or O_2 molecules. Therefore, the O–O bond length of isolated O_2 calculated by BS-opt B3LYP method involved no spin contamination error. The results of BS-opt calculations using B3LYP are summarized in Table 1. The binding energy between Au and O_2 by BS-opt was 1.55 kcal/mol. The O–O bond length became slightly longer than that of the O–O

Table 1
Calculation results for Au–O_2 by BS-opt and AP-opt B3LYP methods.

	BS-opt B3LYP	AP-opt B3LYP	Difference[a]
R(Au–O)[b]	2.447	2.359	−0.088
R(O–O)[b]	1.230	1.237	+0.007
A(Au–O–O)[c]	119.50	119.33	−0.168
Binding energy[d]	1.55	3.76	+2.21

[a] Difference between BS-opt and AP-opt results.
[b] Bond distance in Å.
[c] Angle in degrees.
[d] Binding energy in kcal/mol.

Table 2
Calculation results for neutral, cationic, and anionic Au_2–O_2 models by BS-opt B3LYP method.

	Spin state	Energy[a]	$\langle S^2 \rangle$	Spin density (charge density)				E_{ad}[b]
				Au1	Au2	O1	O2	
Au_2O_2	Triplet	−421.278239	2.0108	0.07(−0.09)	0.01(0.00)	0.90(−0.01)	1.02(−0.10)	2.72
$Au_2O_2^+$	Doublet	−420.939755	1.7305	−0.45(0.45)	−0.42(0.30)	0.80(0.03)	1.07(0.22)	7.76
$Au_2O_2^-$	Doublet	−421.385619	0.7649	−0.04(−0.40)	−0.02(−0.07)	0.44(−0.32)	0.61(−0.20)	23.3
Au_2	Singlet	−270.948416	0.0000	0.00(0.00)	0.00(0.00)	–	–	–
Au_2^+	Doublet	−270.601929	0.7598	0.50(0.50)	0.50(0.50)	–	–	–
Au_2^-	Doublet	−271.022951	0.7563	0.50(−0.50)	0.50(−0.50)	–	–	–
O_2	Triplet	−150.325484	2.0089	–	–	1.00(0.00)	1.00(0.00)	–

[a] Total energy in a.u.
[b] Adsorption energy in kcal/mol.

Table 3
Optimized geometries for the Au_2–O_2 and Au_2^-–O_2 models by BS-opt.

	Au_2–O_2	Au_2^-–O_2
	BS-opt	BS-opt
R(Au–Au)[a]	2.566	2.625
R(Au–O)[a]	2.469	2.152
R(O–O)[a]	1.220	1.316
A(Au–Au–O)[b]	179.76	177.21
A(Au–O–O)[b]	120.94	116.42
D(Au–Au–O–O)[c]	47.04	−178.65

[a] Distance in Å.
[b] Angle in degrees.
[c] Dihedral angle in degrees.

bond length in isolated O_2, as the O–O distance in isolated O_2 calculated by B3LYP method was 1.215 Å. The results of our approximate spin-projected broken symmetry geometry optimization (AP-opt) calculation using B3LYP are also summarized in Table 1. The binding energy calculated by AP-opt B3LYP was larger than that calculated by BS-opt B3LYP, as the binding energy between Au and O_2 by AP-opt B3LYP was 3.76 kcal/mol. The optimized bond length between Au and O from AP-opt was shorter than that obtained by BS-opt, while the optimized O–O distance in the Au–O_2 model by AP-opt was longer than that found by BS-opt. Therefore, both the adsorption energy and the optimized geometry of Au–O_2 were greatly changed by the elimination of spin contamination error from the results of BS-opt calculations. For small organic molecules, such as CH_2 radical, we have confirmed the validity of the AP-opt method. However, it is currently difficult to carry out accurate *ab initio* symmetry-adapted methods, such as CASPT2. The comparison of optimized geometries of Au–O_2 from AP-opt B3LYP to those obtained from an accurate *ab initio* symmetry-adapted method is the next task.

Next, Au_2–O_2, Au_2^+–O_2, and Au_2^-–O_2 models were investigated by BS-opt B3LYP. The results are summarized in Tables 2–5, and Fig. 1. The ground spin states of isolated Au_2, Au_2^+, and Au_2^- clusters are singlet, doublet, and doublet, respectively. The ground spin states of Au_2–O_2, Au_2^+–O_2, and Au_2^-–O_2 model systems were determined to be triplet, doublet, and doublet, respectively. The obtained optimized geometries of Au_2–O_2, Au_2^+–O_2, and Au_2^-–O_2 models had similar geometries. As the spin state of Au_2 was singlet, Au_2 had a closed shell electronic state. Therefore, the binding energy of Au_2–O_2 is the lowest of the three models examined. The schematic structure is depicted in Fig. 1(b) and the detailed geometric parameters are summarized in Tables 3 and 5. The Mulliken population analyses for Au_2–O_2 and Au_2^-–O_2 models summarized in Table 2 show that the spin density was localized on the O_2 molecule. This indicates that the spin densities on Au_2^- in the Au_2^-–O_2 model system vanished, although isolated Au_2^- and O_2 have open-shell electronic states. This is due to charge transfer

Table 4
Calculation results for the Au_2^+–O_2 model by BS-opt and AP-opt B3LYP.

Model	Method (spin state)	BS-opt (doublet)		BS-opt (quartet)		AP-opt (doublet)
		Total energy[a]	$\langle S^2 \rangle$	Total energy[a]	$\langle S^2 \rangle$	Total energy[a]
Au_2^+–O_2	Type I	−420.939755	1.7305	−420.939147	3.7671	−420.939846
	Type II	−420.938393	1.5873	−420.931834	3.7663	−420.940913

[a] Total energy in a.u.

Table 5
Optimized geometries and binding energies for the Au_2^+–O_2 model by BS-opt and AP-opt B3LYP.

	Type I			Type II		
	BS-opt	AP-opt	Variation[a]	BS-opt	AP-opt	Variation[a]
R(Au–Au)[b]	2.692	2.691	−0.001	2.691	2.684	−0.007
R(Au–O)[b]	2.405	2.404	−0.001	2.448	2.409	−0.039
R(O–O)[b]	1.213	1.212	−0.001	1.211	1.209	−0.002
A(Au–Au–O)[c]	170.42	168.22	−2.20	110.23	103.82	−6.43
A(Au–O–O)[c]	125.52	126.28	+0.76	117.21	115.54	−1.67
D(Au–Au–O–O)[d]	0.33	0.92	+0.59	180.0	180.0	0.00
Binding energy[e]	7.66	7.85	+0.19	7.02	8.77	+1.75

[a] Difference between the results of BS-opt and AP-opt.
[b] Distance in Å.
[c] Angle in degrees.
[d] Dihedral angle in degrees.
[e] Binding energy in kcal/mol.

Table 6
Calculation results for the Au_{13}–O_2 model by BS-opt and AP-opt B3LYP.

		Spin state	Total energy[a]	$\langle S^2 \rangle$	R(Au–O)[b]	R(O–O)[b]	A(Au–O–O)[c]	Binding energy[d]
BS-opt	O_2	Triplet	−150.325484	2.0089	–	1.215	–	–
	Au_{13}	Sextet	−1761.379416	8.7625	–	–	–	–
	Au_{13}–O_2	Quartet	−1911.709034	5.4547	2.419	1.239	119.9	2.59
AP–opt	Au_{13}–O_2	Quartet	−1911.710673	–	2.365	1.252	119.4	3.65

[a] Total energy in a.u.
[b] Length in Å.
[c] Angle in degrees.
[d] Binding energy in kcal/mol.

Table 7
Calculation results for the Au_{13}–O_2 model by BS-opt B3LYP.

	Spin density (charge density)		
	Au[a]	O1	O2
$Au_{13}O_2$	0.248(−0.577)	−0.832(0.005)	−0.932(−0.014)
Au_{13}	0.371(−0.621)	–	–

[a] The Au atom directly bound to O_2 molecule.

from Au_2^- to O_2 in the Au_2^-–O_2 model system. Furthermore, the Mulliken population analysis for Au_2^+–O_2 model determined that the spin densities on both Au_2^+ and O_2 in the Au_2^+–O_2 model system were retained. Therefore, the spin contamination error in the Au_2–O_2 and Au_2^-–O_2 models was negligible, as the deviation of calculated $\langle S^2 \rangle$ values from exact values was very small. On the other hand, the calculation results for the Au_2^+–O_2 model contained large spin contamination error, as the calculated $\langle S^2 \rangle$ value was 1.731. Therefore, the AP-opt calculation was applied to the Au_2^+–O_2 model, and AP-opt B3LYP results are displayed in Fig. 1, Tables 4 and 5. Two stable structures (types I and II) with doublet spin state, shown in Fig. 1, were obtained. As mentioned previously, the calculation results suggest that the most stable doublet structure calculated by the BS-opt method was the type I structure depicted in Fig. 1(b). However, we found that the type II structure displayed in Fig. 1(c) was the most stable doublet structure according to AP-opt. The elimination of the spin contamination error from the BS-opt calculations for the model systems is important for theoretical investigation of the characteristics of model systems containing open shell precious metal clusters, and the AP-opt method effectively eliminated the spin contamination error from the obtained broken symmetry wavefunction and the calculated energy.

Finally, the Au_{13}–O_2 model system was investigated. The results are summarized in Tables 6 and 7. The calculated $\langle S^2 \rangle$ value of Au_{13}–O_2 by BS-opt contained a large spin contamination error, as the $\langle S^2 \rangle$ value of the Au_{13}–O_2 model system is 5.4547. Additionally, there are localized spins on Au atoms directly bound to O_2 molecules, and O atoms in O_2 molecules, within the Au_{13}–O_2 system, as shown in Table 7. Therefore, AP-opt was applied to the Au_{13}–O_2 model system. Comparing with the results of BS-opt and AP-opt methods, elimination of the spin contamination from the BS-opt calculation shortened the Au–O bond and lengthened the O–O bond. The binding energy between Au_{13} and O_2 calculated by AP-opt was larger than that calculated by BS-opt. This tendency is similar to those of the Au–O_2 and Au_2^+–O_2 model systems. Consequently, we conclude that the AP-opt method is indispensable for the detailed investigation of open shell cluster model catalysts. Additionally, the AP-opt method is applicable to other model systems containing open shell precious metal clusters.

4. Conclusion

The present theoretical calculations have provided the following interpretations of the interaction between oxygen molecules and small Au clusters.

(1) Both adsorption energies and optimized geometries for model systems containing Au clusters were greatly changed by the elimination of spin contamination error from BS-opt calculation results.
(2) The AP-opt method effectively eliminated the spin contamination from the obtained broken symmetry geometry and the calculated energy.
(3) The AP-opt method is indispensable for the detailed investigation of open shell cluster model systems.

Acknowledgements

This work was supported by JST, CREST, and a Grant in-Aid for Scientific Research from the Ministry of Education, Culture, Sports, Science, and Technology of Japan.

References

[1] M. Haruta, N. Yamada, T. Kobayashi, S. Iijima, J. Catal. 115 (1989) 301.
[2] M. Haruta, S. Tsubota, T. Kobayashi, H. Kageyama, M.J. Genet, B. Delmon, J. Catal. 144 (1993) 175.
[3] M. Okumura, S. Nakamura, S. Tsubota, T. Nakamura, M. Azuma, M. Haruta, Catal. Lett. 51 (1998) 53.
[4] M. Okumura, S. Tsubota, M. Iwamoto, M. Haruta, Chem. Lett. (1998) 315.
[5] M. Okumura, Y. Kitagawa, K. Yamaguchi, M. Haruta, Chem. Phys. Lett. 346 (2001) 163.
[6] M. Okumura, Y. Kitagawa, M. Haruta, K. Yamaguchi, Appl. Catal. A 291 (2005) 37.
[7] Y. Negishi, Y. Takasugi, S. Sato, H. Yao, K. Kimura, T. Tsukuda, J. Am. Chem. Soc. 126 (2004) 6518.
[8] H. Tsunoyama, H. Sakurai, Y. Negishi, T. Tsukuda, J. Am. Chem. Soc. 127 (2005) 9374.
[9] X. López, M.-Y. Huang, G.-C. Huang, S.-M. Peng, F.-Y. Li, M. Bénard, M.-M. Rohmer, Inorg. Chem. 45 (2006) 9075.
[10] K. Yamaguchi, in: R. Carbo, M. Klobukowski (Eds.), Self-consistent Field Theory and Applications, Elsevier, Amsterdam, 1990, p. 727.
[11] K. Yamaguchi, T. Kawakami, Y. Takano, Y. Kitagawa, Y. Yamashita, H. Fujita, Int. J. Quantam Chem. 90 (2002) 370.
[12] K. Yamaguchi, Y. Takahara, T. Fueno, K.N. Houk, Theor. Chim. Acta 73 (1988) 337.
[13] S. Yamanaka, M. Okumura, M. Nakano, K. Yamaguchi, J. Mol. Struct. (Theochem.) 310 (1994) 205.
[14] Y. Kitagawa, T. Saito, M. Ito, M. Shoji, K. Koizumi, S. Yamanaka, T. Kawakami, M. Okumura, K. Yamaguchi, Chem. Phys. Lett. 442 (2007) 445.
[15] Y. Kitagawa, T. Saito, M. Ito, M. Shoji, K. Koizumi, S. Yamanaka, T. Kawakami, M. Okumura, K. Yamaguchi, Int. J. Quantam Chem. 107 (2007) 3094.
[16] A. Szabo, N.S. Ostlund, Modern Quantum Chemistry, Dover Publications, Inc., New York, NY, 1996, pp. 205–230 (Chapter 3).
[17] D. Gatteschi, O. Kahn, J.S. Miller, F. Palacio, Magnetic Molecular Materials, Kluwer Academic Publishers, Dordrecht, 1991.
[18] O. Kahn, Magnetism: A Supermolecular Function, NATO ASI Series C, vol. 484, Kluwer Academic Publishers, Dordrecht, 1996.
[19] G. Fogarasi, X. Zhou, P.W. Taylor, P. Pulay, J. Am. Chem. Soc. 114 (1992) 8191.
[20] M.J. Frisch, et al., Gaussian 03, Revision D.01, Gaussian, Inc., Wallingford, CT, 2004